Contents lists available at ScienceDirect

NeuroImage: Clinical

Diffusion spectrum imaging of patients with middle cerebral artery stenosis

Xinghua Wan [a,1], Yu Xiao [b,1], Zhenghua Liu [c,*]

[a] *The Department of Radiology, The People's Hospital of Nanchang County, China*
[b] *Medical College of Nanchang University, People's Hospital of Jiangxi Province, China*
[c] *Medical Imaging Center, Affiliated Hospital of Jiangxi University of Traditional Chinese Medicine, China*

A R T I C L E   I N F O

A B S T R A C T

Objective: We aimed to detect microstructural changes in the brains of patients with unilateral middle cerebral artery (MCA) stenosis and to assess the integrity of the fiber structure and the small-world networks using diffusion spectrum imaging (DSI).

Methods: A total of 21 healthy controls and 48 patients with unilateral MCA stenosis underwent 3.0 T MRI examination using DSI technique. Differential tractography, diffusion connectometry, and structural networks were performed by using DSI software. The correlation between the stenosis and quantitative anisotropy (QA) were analyzed using multiple regression models in the correlation tractography.

Results: Differential tractography analysis showed that the left or right MCA stenosis group had decreased fiber connectivity in the brain network compared with the control group. The correlation tractography analysis of the patients with MCA stenosis showed that QA was negatively correlated with stenosis in the bilateral arcuate fasciculus, bilateral corticostriatal and corticothalamic pathway, bilateral corticopontine and corticospinal tract, right superior longitudinal fasciculus, right cingulum, corpus callosum, and left frontal aslant tract. Statistically significant differences were shown between the MCA stenosis groups and control group in graph density, global efficiency, network path length, and rich club coefficient.

Conclusion: DSI revealed that stroke-free patients with unilateral MCA stenosis have a disrupted structural network and damaged white matter fibers. Furthermore, the fiber connection disruption is more severe in the ipsilateral hemisphere and less prominent in the contralateral hemisphere in patients with unilateral MCA stenosis. Therefore, microstructural impairment has happened to patients with unilateral MCA stenosis even at a subclinical stage.

1. Introductions

Following the clinical application of diffusion-weighted imaging (DWI), diverse models, such as diffusion spectrum imaging (DSI) and diffusion tension imaging (DTI), have been created to calculate diffusion parameters (Chang et al., 2017; Yeh et al., 2011; Dell'Acqua and Tournier, 2019; Bigham et al, 2020; Sexton et al, 2011). These diffusion-imaging techniques each have their own advantages.

The most important parameter in DSI is quantitative anisotropy (QA). QA represents the number of anisotropic spins from the peak orientations according to a spin distribution function in generalized q-sampling imaging (Yeh et al., 2011; Dell'Acqua and Tournier, 2019). Furthermore, it can also undergo differential tractography, diffusion

connectometry, and structural networks (Yeh et al., 2016, 2019; Wang et al., 2018). The DSI technique can perform QA-aided tractography, which has been proven to outperform DTI using fiber tractography and is less susceptible to crossing fibers (Yeh et al., 2016). DSI has been applied in the research of cerebral conditions, such as chronic stoke, seizure and mild traumatic brain injury (Yeh et al., 2013; Li et al., 2022; da Silva et al., 2020).

Some researchers have proven that structural and functional networks exist in the human brain and hold "small-world" properties. Small-world networks possess a low path length, high clustering coefficient, and a rich club structure, thereby allowing the brain to work more effectively at minimal cost. However, healthy participants of different ages and intelligence have different performances in small-

world networks (Li et al., 2009; Gong et al., 2009). DSI and DTI can display structural networks (Wang et al., 2018; Dai et al., 2019). Several studies have discovered disrupted small-world networks in Alzheimer's disease (AD) using diffusion magnetic resonance imaging (MRI) (Dai et al., 2019).

Large vessel diseases can lead to cortical and subcortical infarcts, which affect functional brain regions and result in vascular cognitive impairment (Frantellizzi et al., 2020). However, chronic occlusion of a large vessel may not lead to brain infarcts because collateral circulation develops in these ischemic regions. Therefore, if there is no brain infarct, abnormal appearances during chronic middle cerebral artery (MCA) occlusion can only be revealed via advanced imaging, such as via an arterial spin labeling sequence (Liu and Li, 2016). Previous research indicates that abnormal DTI performance is related to neurocognitive decline at a subclinical stage in patients with presymptomatic carotid stenosis (Lin et al., 2014). However, no studies have shown abnormal changes in the white matter of stroke-free patients with unilateral MCA stenosis or occlusion by using DTI or DSI. We hypothesized that stroke-free patients with unilateral MCA stenosis may have microstructural impairment at a subclinical stage. Therefore, this study was conducted to detect microstructural performance in the brain of patients with unilateral MCA stenosis and to assess the integrity of the fiber structure and small-world networks using DSI.

2. Materials and methods

2.1. Subjects

This prospective study was approved by the institutional ethical committee. Informed consent was obtained from each participant prior to inclusion in the study.

A total of 21 healthy subjects and 77 patients with MCA stenosis or occlusion were included. Each patient underwent clinical evaluations, MRI examinations, and cervical vascular color ultrasonic inspections. The inclusion criteria were as follows: 1) unilateral MCA M1 segment stenosis or occlusion, 2) no stenosis in the bilateral cervical vasculature, 3) no brain surgery, 4) no brain motion artifacts in DSI, and 5) no stroke. Five and three patients were excluded because of bilateral MCA stenosis and motion artifacts, respectively. Twenty-one patients were excluded because of common carotid artery or internal carotid artery stenosis, which was detected using color Doppler ultrasonography. Subsequently, 21 healthy participants and 48 patients with MCA stenosis or occlusion were recruited for the study. Fig. 1 shows the flowchart of inclusion and

exclusion criteria.

2.2. Image acquisition and processing

All patients underwent 3.0 T MRI examination (Ingenia Elition X; Philips Medical Systems, Netherlands). A 16-channel head coil was used to acquire the image signal. The MRI protocols included DSI, three-dimensional (3D) MR angiography (MRA), high-resolution T2-weighted imaging (T2WI) and DWI. The high-resolution T2WI sequence was located on the stenotic M1 segment of the MCA in perpendicular direction, which shown on 3D MRA. The 120-direction DSI protocol was as follows: field of view, 240×240 mm^2; repetition time, 5000 ms; echo time, 80 ms; voxel size, $1.2 \times 1.2 \times 1.2$ mm^3; 10 different b values with a maximum of 4000 s/mm^2. The parameters of other MRI protocols were shown in Appendix Table E1.

Before the DSI data were processed, the FMRIB Software Library was used to correct for eddy current to reduce eddy current artifacts. DSI data were processed using DSI Studio software (Yeh, https://dsi-studio.labsolver.org/).

Unilateral MCA stenosis of the patients included occlusion or severe stenosis (<50 % lumen diameter). The stenosis degree was calculated as the diameter of the maximal vessel narrowing relative to the normal proximal lumen diameter on high-resolution T2WI. Two examples of MCA stenosis and occlusion were shown in Appendix Fig. E1 and E2, respectively. The patients were divided into left MCA and right MCA stenosis groups, based on the location of MCA narrowing.

2.3. Group differential tractography

Q-space diffeomorphic reconstruction (QSDR) was used to reconstruct the DSI in the Montreal Neurological Institute template, which has a resolution of 2 mm. DSI data from the controls and the patients with unilateral MCA stenosis were then averaged into a template. We constructed three group average templates for the healthy control group and left or right MCA stenosis patient groups (21 healthy subjects, 22 patients with left stenotic MCA, and 26 patients with right stenotic MCA) by averaging the spin distribution function. Angular threshold and step size were set to 90° and 1.2 mm, respectively. Topology-informed pruning was set to 6 iterations. The increased and decreased anisotropy were calculated based on minimum length of 20 mm and differential tracking threshold of 0.2, respectively. 20 % was applied for the threshold of significantly decreased QA (Sihvonen et al., 2021).

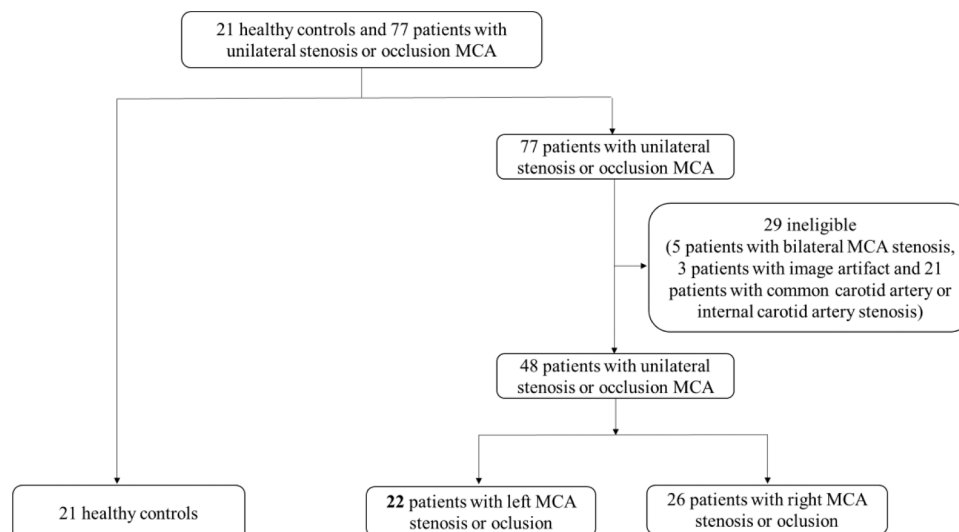The connectivity matrix was obtained using a total of 1,000,000

Fig. 1. Flowchart shows inclusion and exclusion criteria.

seeds in the white matter based on the FreeSurferDKT cortical atlas. A connectogram was plotted to visualize the differences between the average templates of the stenosis groups and the control group.

2.4. Correlation tractography

First, we created the left and the right stenotic MCA connectometry database (21 controls and 22 patients with left stenosis MCA; 21 controls and 26 patients with right stenosis MCA) according to the QSDR. Second, The QA of fibers were regressed with stenosis, sex, and age using a multiple linear regression model. DSI Studio can find any tracks correlated with stenosis. The effect of other covariates including sex and age can be regressed out using a linear regression model (Yeh, https://dsi-studio.labsolver.org/doc/gui_cx.html). During the analysis, T thresholds of 3.0, a false discovery rate (FDR) of 0.05, and other default parameters such as permutation count were used. Third, fiber tractography was performed using a total of 1,000,000 seeds in the whole-brain and a deterministic fiber tracking algorithm based on the default values of parameters, such as the anisotropy threshold and angular threshold. Fourth, the connectivity matrix was calculated based on the FreeSurferDKT cortical atlas. Then, the small-worldness parameters of the network were obtained from the connectivity matrix.

2.5. Statistical analysis

Pearson's chi-square test was used to analyze categorical variables among the controls and the left and right MCA stenosis patients. Independent t-tests were used to analyze the parameters of the small-worldness network, such as the clustering coefficient, network path, small-worldness, global efficiency and rich club, between the patients and controls using SPSS software (Version 25.0; IBM, Armonk, NY). Statistical significance was set at $P < 0.05$. The QA of fibers were correlated with stenosis, sex, and age using a multiple linear regression model. The FDR correction was 0.05.

3. Results

The patients' demographic information and medical comorbidities are listed in Table 1. A total of 21, 22 and 26 patients were included in the control group and the left and right MCA stenosis groups, respectively. Eighteen and nineteen patients had occluded MCA in the left and right MCA stenosis groups, respectively (Table 1). The degree of MCA narrowing of 4 and 7 patients is 0.24 ± 0.04 and 0.20 ± 0.06 in the left and right MCA stenosis groups, respectively, on the high-resolution T2WI images.

3.1. Group average connectogram

Fig. 2 illustrates the average connectograms of the control group and the left and right MCA stenosis groups. The left and right parts of the connectogram correspond to the left and right hemisphere, respectively. The group-average connectogram revealed minor differences. Fig. 3A and 3B show the differences between the connectogram of patients with

the left or right MCA stenosis and controls. Fig. 3 indicates a substantial amount of intra-hemisphere white matter fiber dysconnectivity and shows that the lesion area was larger than the contralateral area, which indicated that the fiber connection disruption was more severe in the ipsilateral hemisphere and less prominent in the contralateral hemisphere. Furthermore, fiber connection disruption was not found in the inter-hemisphere decussating fibers (Fig. 3).

3.2. Differential tractography

The left MCA stenosis group had decreased fiber connectivity in the brain network (fiber mean length = 23.3 mm, fiber count = 1663) compared with the control group. Decreased QA (>20 %) was observed in the bilateral superior longitudinal fasciculus, bilateral parietal aslant tract, left frontal aslant tract, left middle longitudinal fasciculus, left parahippocampal cingulum, right anterior and superior corticostriatal tract, right posterior thalamic radiation, and right uncinate fasciculus (Fig. 4A and B).

The right MCA stenosis group had decreased fiber connectivity in the brain network (fiber mean length = 22.7 mm, fiber count = 900) compared with the control group. Decreased QA (>20 %) was observed in the forceps major of the corpus callosum, bilateral superior and left middle longitudinal fasciculus, left frontal aslant tract, left arcuate fasciculus, left vertical occipital fasciculus, right superior corticostriatal tract, right uncinate fasciculus, and right posterior thalamic radiation (Fig. 4C and D).

3.3. Correlation tractography

The correlation tractography analysis of patients with left MCA stenosis showed that QA was negatively (FDR < 0.05) correlated with stenosis in the corpus callosum, bilateral corticostriatal and corticothalamic pathway, bilateral cingulum, bilateral corticopontine and corticospinal tract, bilateral superior longitudinal fasciculus, bilateral inferior fronto-occipital fasciculus, left frontal aslant tract, left arcuate fasciculus, and right reticulospinal tract (Fig. 5A and B).

Connectometry analysis of patients with right MCA stenosis showed that QA was negatively correlated with stenosis in the bilateral corticothalamic and corticostriatal pathway, bilateral corticopontine and corticospinal tract, bilateral arcuate fasciculus, right superior and middle longitudinal fasciculus, right cingulum, right reticulospinal tract, right fornix, left extreme capsule, left frontal aslant tract, and corpus callosum (Fig. 5C and 5D). The correlation of stenosis severity with QA of each fiber in left or right MCA stenosis group were shown in Appendix Table E2 and E3, respectively.

QA of patients with left or right MCA stenosis was negatively (FDR < 0.05) correlated with stenosis in white matter anomalies. Fig. 6 shows the connectivity matrix obtained from the white matter anomalies of the left or right MCA stenosis groups based on the FreeSurferDKT cortical atlas.

3.4. Network measures

Significant differences were shown between the left MCA stenosis group and control group in graph density, global efficiency (binary), network path length (binary), and rich club coefficient (binary: k = 5, 10; weighted: 15, 20, 25). We also found significant differences between the right MCA stenosis group and the control group in graph density, network path length (binary), small-worldness coefficient (binary), global efficiency (binary), and rich club coefficient (binary: k = 5, 10; weighted: 20, 25). Table 2 shows the results of the small-worldness network between the left and right MCA stenosis group and the control group.

Table 1
Demographic data of the controls and severe stenotic and occluded MCA patients.

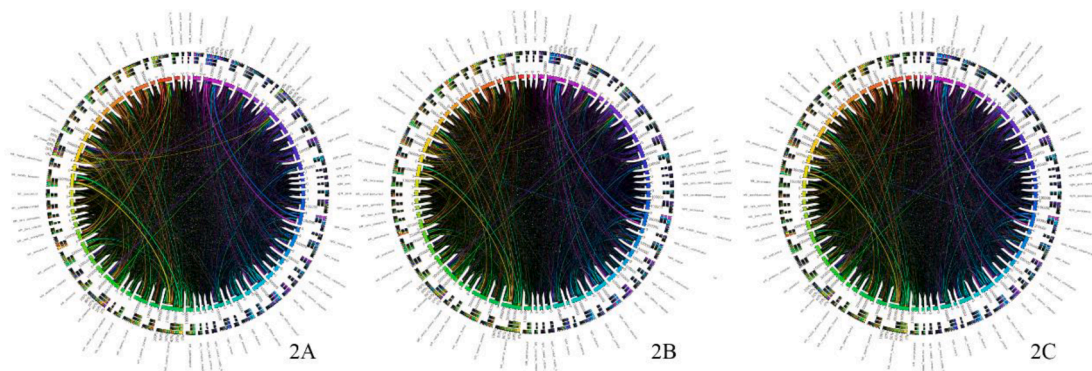|	Controls (n=21)	Left MCA stenosis (n = 22)	Right MCA stenosis (n = 26)	P value
Female	10	5	8	0.210
Age	63.1 ± 6.7	64.9 ± 9.2	61.4 ± 5.5	0.243
Hypertension	8	12	14	0.470
Type 2 diabetes	5	8	11	0.409
Occluded MCA	0	18	19	0.159

Fig. 2. Group average connectogram of the control group (A), the left (B) and the right (C) MCA stenosis patient groups.
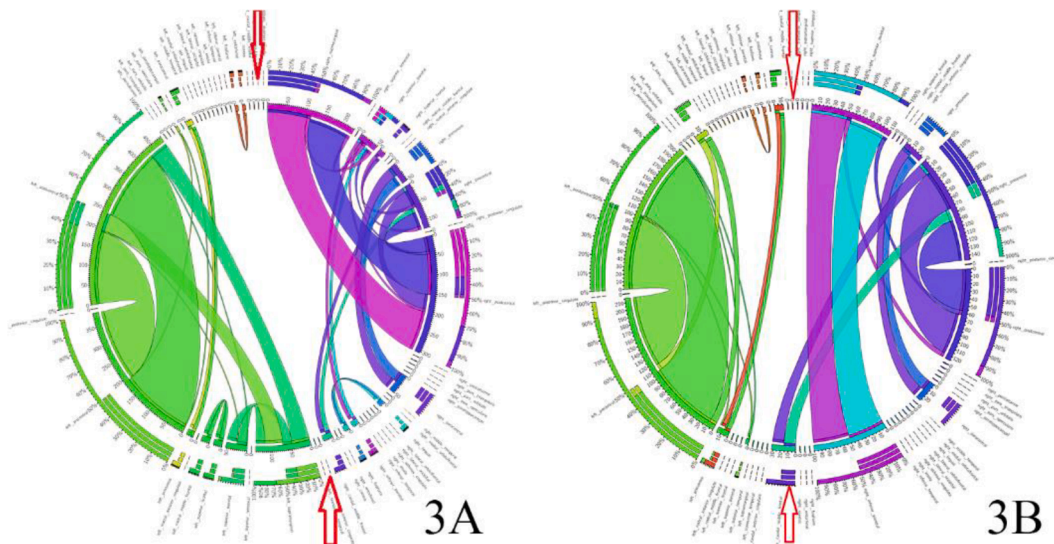

Fig. 3. Connectogram of dysconnectivity between the control and the left (A) or the right (B) MCA group-average templates shows that the dysconnectivity involves multiples pathways. The red arrow indicates the boundary between the two hemispheres of the brain. It indicated that the fiber connection disruption was more severe in the ipsilateral hemisphere and less prominent in the contralateral hemisphere. Furthermore, fiber connection disruption was not found in the inter-hemisphere decussating fibers. (For interpretation of the references to color in this figure legend, the reader is referred to the web version of this article.)
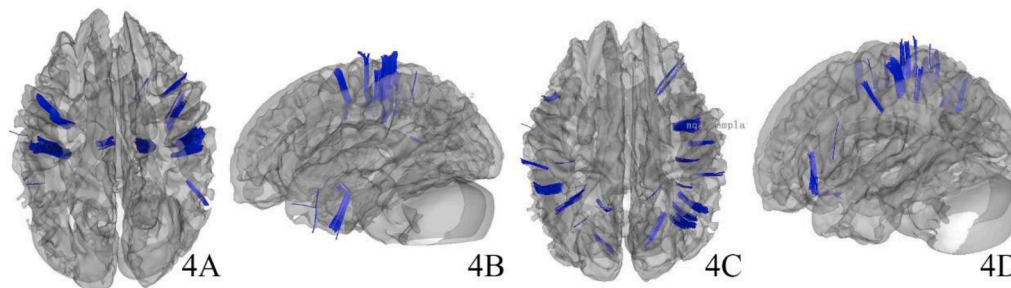

Fig. 4. Differential tractography results between the control and the left (A and B) or the right (C and D) MCA group-average templates. Structural white matter anomalies marked by decreased QA (>20 %) in the left or the right MCA group-average templates.

4. Discussions

Several studies have indicated changes in the white matter fibers after stroke (Luijten et al., 2021; Sagnier et al., 2020). However, none have shown abnormal performances in the white matter fibers of patients without stroke after chronic MCA occlusion. In the study, DSI revealed that stroke-free patients with unilateral MCA stenosis have a damaged white matter fiber bundle and disrupted structural network.

Connectograms are useful for detecting neuronal injury (Yeh et al.,

2019). Connectogram analysis revealed differences between the average templates of the stenosis groups and the control group. The results indicated that the fiber connection disruption is more severe in the ipsilateral hemisphere and less prominent in the contralateral hemisphere. Furthermore, fiber connection disruption was not found in the inter-hemispheric decussating fibers. Therefore, we observed differences in the intra-hemispheric fibers and none in the inter-hemispheric fibers (Fig. 3). From the connectogram analysis, we obtained fibers with decreased QA, which were further categorized based on the location of
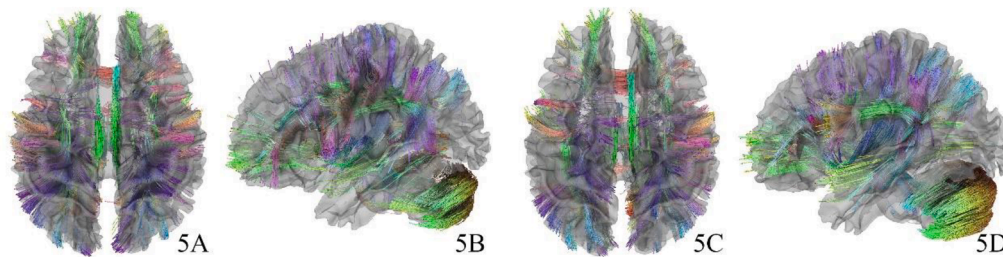
Fig. 5. Connectometry analysis shows significant correlation between stenosis and quantitative anisotropy in the left (A and B) or right (C and D) MCA stenosis groups.
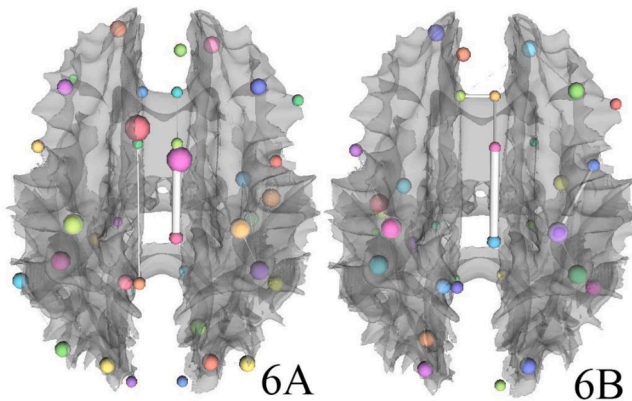

Fig. 6. Correlation tractography analysis of the patients with the left or right MCA stenosis showed that QA was positively (FDR < 0.05) correlated with stenosis in white matter anomalies. The connectivity matrix of the left (A) or right (B) MCA stenosis groups was obtained using the white matter anomalies based on the FreeSurferDKT cortical atlas.

Table 2

Statistical results of the independent t test for the parameters of the small-worldness network between the left or right MCA stenosis group and the control group.

	Left MCA group	Left MCA group	Control group
Density	0.55 ± 0.04*	0.54 ± 0.05*	0.58 ± 0.05
Clustering coff (B)	0.79 ± 0.02	0.79 ± 0.02	0.80 ± 0.02
Clustering coff (W)	0.03 ± 0.004	0.03 ± 0.005	0.03 ± 0.005
Transitivity (B)	0.16 ± 0.02	0.17 ± 0.02	0.16 ± 0.03
Transitivity (W)	0.03 ± 0.003	0.03 ± 0.004	0.03 ± 0.005
Path Length (B)	1.47 ± 0.04*	1.49 ± 0.06*	1.43 ± 0.06
Path Length (W)	11.8 ± 1.02	11.9 ± 2.10	12.0 ± 2.22
Small-Worldness (B)	0.54 ± 0.02	0.53 ± 0.03*	0.56 ± 0.04
Small-Worldness (W)	0.003 ± 0.0005	0.003 ± 0.0007	0.003 ± 0.0008
Global efficiency (B)	0.76 ± 0.02*	0.75 ± 0.03*	0.78 ± 0.03
Global efficiency (W)	0.11 ± 0.01	0.11 ± 0.02	0.11 ± 0.02
Assortativity (B)	-0.04 ± 0.03	-0.04 ± 0.04	-0.04 ± 0.04
Assortativity (W)	-0.08 ± 0.02	-0.08 ± 0.03	-0.07 ± 0.02
Rich club K5 (B)	0.55 ± 0.04*	0.54 ± 0.05*	0.58 ± 0.05
Rich club K10 (B)	0.55 ± 0.04*	0.54 ± 0.04*	0.58 ± 0.05
Rich club K15 (B)	0.60 ± 0.03	0.58 ± 0.05	0.61 ± 0.05
Rich club K20 (B)	0.69 ± 0.02	0.68 ± 0.04	0.69 ± 0.03
Rich club K25 (B)	0.79 ± 0.02	0.77 ± 0.03	0.77 ± 0.03
Rich club K5 (W)	1.00 ± 0.00	1.00 ± 0.00	1.00 ± 0.00
Rich club K10 (W)	1.00 ± 0.00	1.00 ± 0.00	1.00 ± 0.00
Rich club K15 (W)	0.95 ± 0.04*	0.95 ± 0.04*	0.97 ± 0.03
Rich club K20 (W)	0.85 ± 0.05*	0.83 ± 0.07*	0.89 ± 0.05
Rich club K25 (W)	0.73 ± 0.06*	0.72 ± 0.08*	0.78 ± 0.08

An asterisk (*) indicates that p values between the MCA stenosis group and control group is lower than 0.05. B is binary and W is weighted.

the fiber connecting to the frontal lobe and limbic system or temporal lobe (Fig. 4). The frontal aslant tract, uncinate fasciculus, and superior and middle longitudinal fasciculus are connected to the frontal lobe and correlated with cognition and sentiment (Blair et al., 2020; Dricu et al., 2020). The superior corticostriatal tract and parahippocampal cingulum belong to the limbic system, which are also correlated with cognition and sentiment. The parietal aslant tract and the forceps major of corpus callosum are connected to the occipital lobe, where the visual cortex is located, and the posterior thalamic radiation and vertical occipital fasciculus are correlated with visual radiation. Therefore, these fibers can affect vision.

In our study, most of the affected fibers in the right MCA stenosis group were similar to those in the left MCA stenosis group. The left vertical occipital fasciculus and left arcuate fasciculus were present in the right MCA stenosis group, but not in the left MCA stenosis group. These fibers are connected to the frontal lobe and correlated with cognition and sentiment. Furthermore, the bilateral parietal aslant tract, right anterior corticostriatal tract, and left parahippocampal cingulum existed in the left MCA stenosis group but not in the right MCA stenosis group.

Correlation tractography analysis showed decreased QA in the bilateral arcuate fasciculus, bilateral corticostriatal and corticothalamic pathway, bilateral corticopontine and corticospinal tract, right superior longitudinal fasciculus, right cingulum, corpus callosum, and left frontal aslant tract for the left or right MCA group compared to the control group (Fig. 5). The Corticostriatal and corticothalamic pathways are related to cognition and sentiment. The superior longitudinal fasciculus, corpus callosum, cingulum, arcuate fasciculus, and frontal aslant tract are connected to the frontal lobe; thus, they are correlated with cognition and sentiment. The corticopontine tract is involved in movement. Furthermore, the affected fibers in the left MCA stenosis group comprised of the bilateral inferior fronto-occipital fasciculus and left arcuate fasciculus, which are related to the frontal lobe. Therefore, they are correlated with cognition and sentiment. Moreover, the affected fibers in the right MCA stenosis group comprised of the right fornix and left extreme capsule. They are efferent fibers of the hippocampus and insula, which belong to the limbic system. Therefore, these fibers are related to cognition and sentiments. Fig. 6 shows the connectivity matrix obtained from the white matter anomalies of the left or right MCA stenosis groups and shows that the abnormal fiber connections are mainly located in the frontal and temporal lobe.

The damaged fibers in this study were the same as those of patients with AD, such as inferior fronto-occipital fasciculi, inferior and superior longitudinal fasciculi, posterior thalamic radiations, hippocampal cingulum, fornix, external capsule, cingulate gyri, corpus callosum, and uncinate fasciculi (Mayo et al., 2016, 2019). Abnormal fibers in the left internal capsule and corona radiata of patients with AD were not found in this study. However, a study reported that patients with AD have abnormal white matter fibers, including the superior and inferior longitudinal fasciculus, uncinate fasciculus, and cingulum (Elahi et al., 2017). All these abnormal tracts were found in patients with MCA stenosis. This may indicate that patients with MCA stenosis have cognitive

impairment.

Previous studies have also indicated significant age- and sex-related effects on the anatomical network and connectivity (Gong et al., 2009, 2011). To better understand the correlation between the stenosis and QA, we removed the effect of age and sex from multiple linear regression models (Yeh, https://dsi-studio.labsolver.org/doc/gui_cx.html).

Group differential tractography can only display the differences in fiber bundles between two groups. However, it cannot reveal what kind of factor cause the differences between them (Yeh et al., 2019). Correlational tractography takes some factors into account and analyzes the correlation among these factors using multiple regression models (Yeh et al., 2016). Therefore, group differential tractography and correlational tractography are two different methods of displaying damaged fiber bundle.

Significant differences were found in the bilateral fiber tracts of the patients with unilateral MCA stenosis. These were consistent with previous studies in which the bilateral tract was affected in patients with unilateral disease (da Silva et al., 2020; Im et al., 2020). This may be due to the following reasons. First, one brain region often gives off bilateral fiber tracts. Second, the fibers can decussate to the contralateral brain region. Therefore, unilateral brain disease often affects bilateral fiber tracts.

The left and right MCA stenosis groups had significantly lower graph density, longer network path length (binary), lower global efficiency (binary), and lower rich club coefficient (binary: k = 5, 10; weighted: k = 20, 25) than the control group (Table 2), which means that it will take more time for the MCA stenosis groups to transmit information than the control group. The rich club hub is an important hub used for information transmission in the brain (Xu et al., 2021). A decreased rich club hub means that some information may not be delivered, and its communication and integration may be damaged. Although the decrease was insignificant in the small-worldness coefficient, the left MCA stenosis group had lower values than the control group. Furthermore, the right MCA stenosis group had significant lower small-worldness (binary) than the control group. Therefore, the MCA stenosis group tended to lose its small-worldness properties. In other words, the left and right MCA stenosis groups had disrupted structural network and rich club organization. In fact, some researchers also indicated that patients with AD and cognitive impairment had disrupted structural networks and club organization by He et al., 2008; Stam et al., 2007; Daianu et al., 2015; Zdanovskis et al., 2021).

This study had some limitations. First, this was a single-center study with a small sample size; multicenter larger-scale studies are desired for validation in the future. Second, some old patients with leukoaraiosis were enrolled. Leukoaraiosis often occurs in old adults, especially in those with cerebrovascular disease. Leukoaraiosis may have influenced some DSI parameters.

5. Conclusions

This study obtained two primary results. First, DSI revealed that stroke-free patients with unilateral MCA stenosis have a disrupted structural network and damaged white matter fibers. The fiber connection disruption is more severe in the ipsilateral hemisphere and less prominent in the contralateral hemisphere. Furthermore, these fibers are connected the frontal and temporal lobe or limbic system. Therefore, microstructural impairment occurs to patients with unilateral MCA stenosis even at a subclinical stage. Second, DSI can detect abnormal anatomic changes in brain tissue microstructure before displaying morphological changes using differential tractography, correlation tractography and network measures. Therefore, DSI is a non-invasive and sensitive tool that can be applied in clinical research.

Ethical approval

All procedures performed in the studies involving human

participants were in accordance with the ethical standards of the institutional and/or national research committee and with the 1964 Helsinki Declaration and its later amendments or comparable ethical standards.

Informed consent

Informed consent was obtained from all individual participants included in the study.

CRediT authorship contribution statement

Zhenghua Liu: Methodology, Conceptualization, Funding acquisition, Software, Writing – original draft, Writing – review & editing.

Declaration of Competing Interest

The authors declare that they have no known competing financial interests or personal relationships that could have appeared to influence the work reported in this paper.

Appendix A. Supplementary data

Supplementary data to this article can be found online at https://doi.org/10.1016/j.nicl.2022.103133.

References

Bigham, B., Zamanpour, S.A., Zemorshidi, F., Boroumand, F., Zare, H., 2020. Alzheimer's disease neuroimaging initiative. identification of superficial white matter abnormalities in alzheimer's disease and mild cognitive impairment using diffusion tensor imaging. J. Alzheimers Dis. Rep. 4 (1), 49–59.

Blair, J.C., Lasiecka, Z.M., Patrie, J., Barrett, M.J., Druzgal, T.J., 2020. Cytoarchitectonic Mapping of MRI detects rapid changes in alzheimer's disease. Front. Neurol. 11, 241.

Chang, E.H., Argyelan, M., Aggarwal, M., Chandon, T.S., Karlsgodt, K.H., Mori, S., Malhotra, A.K., 2017. The role of myelination in measures of white matter integrity: combination of diffusion tensor imaging and two-photon microscopy of CLARITY intact brains. Neuroimage 147, 253–261.

da Silva, N.M., Forsyth, R., McEvoy, A., Miserocchi, A., de Tisi, J., Vos, S.B., Winston, G. P., Duncan, J., Wang, Y., Taylor, P.N., 2020. Network reorganisation following anterior temporal lobe resection and relation with post-surgery seizure relapse: a longitudinal study. Neuroimage: Clin. 27 (102320).

Dai, Z., Lin, Q., Li, T., Wang, X., Yuan, H., Yu, X., He, Y., Wang, H., 2019. Disrupted structural and functional brain networks in Alzheimer's disease. Neurobiol. Aging 75, 71–82.

Daianu, M., Mezher, A., Mendez, M.F., Jahanshad, N., Jimenez, E.E., Thompson, P.M., 2015. Disrupted rich club network in behavioral variant frontotemporal dementia and early-onset Alzheimer's disease. Hum. Brain Mapp. 37, 868–883.

Dell'Acqua, F., Tournier, J.D., 2019. Modelling white matter with spherical deconvolution: how and why? NMR Biomed. 32 (4), e3945.

Dricu, M., Schüpbach, L., Bristle, M., Wiest, R., Moser, D.A., Aue, T., 2020. Group membership dictates the neural correlates of social optimism biases. Sci. Rep. 10 (1), 1139.

Elahi, F.M., Marx, G., Cobigo, Y., Staffaroni, A.M., Kornak, J., Tosun, D., Boxer, A.L., Kramer, J.H., Miller, B.L., Rosen, H.J., 2017. Longitudinal white matter change in frontotemporal dementia subtypes and sporadic late onset Alzheimer's disease. Neuroimage Clin 16, 595–603.

Frantellizzi, V., Pani, A., Ricci, M., Locuratolo, N., Fattapposta, F., De Vincentis, G., 2020. Neuroimaging in vascular cognitive impairment and dementia: a systematic review. J. Alzheimers Dis. 73 (4), 1279–1294.

Gong, G., Rosa-Neto, P., Carbonell, F., Chen, Z.J., He, Y., Evans, A.C., 2009. Age- and gender-related differences in the cortical anatomical network. J. Neurosci. 29 (50), 15684–15693.

Gong, G., He, Y., Evans, A.C., 2011. Brain connectivity: gender makes a difference. Neuroscientist 17 (5), 575–591.

He, Y., Chen, Z., Evans, A., 2008. Structural insights into aberrant topological patterns of large-scale cortical networks in alzheimer's disease. J. Neurosci. 28 (49), 4756–4766.

Im, S., Han, Y.J., Kim, S.H., Yoon, M.J., Oh, J., Kim, Y., 2020. Role of bilateral corticobulbar tracts in dysphagia after middle cerebral artery stroke. Eur. J. Neurol. 27 (11), 2158–2167.

Li, Y., Liu, Y., Li, J., Qin, W., Li, K., Yu, C., Jiang, T., 2009. Brain anatomical network and intelligence. PLoS Comput. Biol. 5 (5), e1000395.

Li, M.J., Yeh, F.C., Huang, S.H., Huang, C.X., Zhang, H., Liu, J., 2022. Differential Tractography and Correlation Tractography Findings on Patients with Mild Traumatic Brain Injury: a Pilot Study. Front. Hum. Neurosci. 16, 751902.

Lin, C.J., Tu, P.C., Chern, C.M., Hsiao, F.J., Chang, F.C., Cheng, H.L., Tang, C.W., Lee, Y. C., Chen, W.T., Lee, I.H., 2014. Connectivity features for identifying cognitive impairment in presymptomatic carotid stenosis. PLoS ONE 9 (1), e85441.

Liu, Z., Li, Y., 2016. Cortical cerebral blood flow, oxygen extraction fraction, and metabolic rate in patients with middle cerebral artery stenosis or acute stroke. AJNR Am. J. Neuroradiol. 37 (4), 607–614.

Luijten, S.P.R., Bos, D., Compagne, K.C.J., Wolff, L., Majoie, C.B.L.M., Roos, Y.B.W.E.M., et al., 2021. Association of white matter lesions and outcome after endovascular stroke treatment. Neurology 96 (3), e333–e342.

Mayo, C.D., Mazerolle, E.L., Ritchie, L., Fisk, J.D., Gawryluk, J.R., 2016. Alzheimer's Disease Neuroimaging Initiative. Longitudinal changes in microstructural white matter metrics in Alzheimer's disease. Neuroimage: Clin 13, 330–338.

Mayo, C.D., Garcia-Barrera, M.A., Mazerolle, E.L., Ritchie, L.J., Fisk, J.D., Gawryluk, J. R., 2019. Alzheimer's disease neuroimaging initiative. Relationship Between DTI metrics and cognitive function in Alzheimer's disease. Front. Aging Neurosci. 10 (436).

Sagnier, S., Catheline, G., Dilharreguy, B., Linck, P.A., Coupé, P., Munsch, F., et al., 2020. Normal-appearing white matter integrity is a predictor of outcome after ischemic stroke. Stroke 51 (2), 449–456.

Sexton C.E., Kalu U.G., Filippini N, Mackay C.E., Ebmeier K.P., 2011. A meta-analysis of diffusion tensor imaging in mild cognitive impairment and Alzheimer's disease. Neurobiol Aging 32(12), 2322.e5-18.

Sihvonen, A.J., Virtala, P., Thiede, A., Laasonen, M., Kujala, T., 2021. Structural white matter connectometry of reading and dyslexia. Neuroimage 241, 118411.

Stam, C.J., Jones, B.F., Nolte, G., Breakspear, M., Scheltens, P., 2007. Small-world networks and functional connectivity in Alzheimer's disease. Cereb. Cortex 17, 92–99.

Wang, H., Wang, Y.H., Fang-Cheng, Y., 2018. Specifying the diffusion MRI connectome in Chinese-speaking children with developmental dyslexia and auditory processing deficits. Pediatr. Neonatol. S1875957218301797-.

Xu, C.X., Jiang, H., Zhao, Z.J., Sun, Y.H., Chen, X., Sun, B.M., et al., 2021. Disruption of rich-club connectivity in cushing disease. World Neurosurg. 148, e275–e281.

Yeh, F.C., Badre, D., Verstynen, T., 2016. Connectometry: a statistical approach harnessing the analytical potential of the local connectome. Neuroimage 125, 162–171.

Yeh F.C., Tang P.F., Tseng W.Y, 2013. Diffusion MRI connectometry automatically reveals affected fiber pathways in individuals with chronic stroke. Neuroimage: Clin 29;2:912-21.

Yeh, F.C., Wedeen, V.J., Tseng, W.Y., 2011. Estimation of fiber orientation and spin density distribution by diffusion deconvolution. Neuroimage 55 (3), 1054–1062.

Yeh, F.C., Zaydan, I.M., Suski, V.R., Lacomis, D., Richardson, R.M., Maroon, J.C., Barrios-Martinez, J., 2019. Differential tractography as a track-based biomarker for neuronal injury. Neuroimage 202, 116131.

Zdanovskis, N., Platkājis, A., Kostiks, A., Karelis, G., Grigorjeva, O., 2021. Brain structural connectivity differences in patients with normal cognition and cognitive impairment. Brain Sci. 11 (7), 943.

Further reading

Yeh, F.C., 2021. DSI Studio (Version 2021 May). Zenodo. https://doi.org/10.5281/zenodo.4764264.